Received: 13 February 2020 | Accepted: 27 October 2020

DOI: 10.1002/hyp.13960

RESEARCH ARTICLE

WILEY

What about reservoirs? Questioning anthropogenic and climatic interferences on water availability

Abdullah Akbas[1,2] | Jim Freer[2,3,4] | Hasan Ozdemir[1] | Paul D. Bates[2,3] | M. Tufan Turp[5,6]

[1]Geography Department, Physical Geography Division, Bursa Uludağ University, Bursa, Turkey

[2]School of Geographical Sciences, University of Bristol, Bristol, UK

[3]Cabot Institute, University of Bristol, Bristol, UK

[4]Centre for Hydrology, University of Saskatchewan, Canmore, Alberta, Canada

[5]Center for Climate Change and Policy Studies, Boğaziçi University, İstanbul, Turkey

[6]Department of Environmental Sciences, Institute of Environmental Sciences, Boğaziçi University, İstanbul, Turkey

Correspondence

Abdullah Akbas, Geography Department, Physical Geography Division, Bursa Uludağ University, Bursa, 16000, Turkey.

Email: abdullahakbas@uludag.edu.tr

Funding information

Bilimsel Araştirma Projeleri Birimi, Istanbul Üniversitesi, Grant/Award Numbers: 57515, 39111, 38985; Türkiye Bilimsel ve Teknolojik Araştirma Kurumu, Grant/Award Number: 2214

Abstract

Water resources in semi-arid regions like the Mediterranean Basin are highly vulnerable because of the high variability of weather systems. Additionally, climate change is altering the timing and pattern of water availability in a region where growing populations are placing extra demands on water supplies. Importantly, how reservoirs and dams have an influence on the amount of water resources available is poorly quantified. Therefore, we examine the impact of reservoirs on water resources together with the impact of climate change in a semi-arid Mediterranean catchment. We simulated the Susurluk basin (23.779-km^2) using the Soil and Water Assessment Tool (SWAT) model. We generate results for with (RSV) and without reservoirs (WRSV) scenarios. We run simulations for current and future conditions using dynamically downscaled outputs of the MPI-ESM-MR general circulation model under two greenhouse gas relative concentration pathways (RCPs) in order to reveal the coupled effect of reservoir and climate impacts. Water resources were then converted to their usages – blue water (water in aquifers and rivers), green water storage (water in the soil) and green water flow (water losses by evaporation and transpiration). The results demonstrate that all water resources except green water flow are projected to decrease under all RCPs compared to the reference period, both long-term and at seasonal scales. However, while water scarcity is expected in the future, reservoir storage is shown to be adequate to overcome this problem. Nevertheless, reservoirs reduce the availability of water, particularly in soil moisture stores, which increases the potential for drought by reducing streamflow. Furthermore, reservoirs cause water losses through evaporation from their open surfaces. We conclude that pressures to protect society from economic damage by building reservoirs have a strong impact on the fluxes of watersheds. This is additional to the effect of climate change on water resources.

KEYWORDS

climate change, Mediterranean, reservoir effect, SWAT, water scarcity

1 | INTRODUCTION

Accessibility and availability of water resources are vital for human activities. Therefore, exploring catchment water balances under environmental change is crucial in terms of water supply, water demand, and water management. Many subcomponents of the hydrological cycle and climate parameters at different spatio-temporal scales are predicted to undergo substantial changes because of intensive greenhouse gas emissions to the atmosphere since industrialization (Arnell & Gosling, 2013; Hagemann et al., 2013; Stocker et al., 2013). Many natural hazards, such as floods and landslides, as well as droughts, will likely increase because of the changing hydrological cycle and its subcomponents (Alfieri, Burek, Feyen, & Forzieri, 2015; Arnell & Gosling, 2013; Dottori et al., 2018; Mueller Schmied et al., 2016; Oki & Kanae, 2006; Samaniego et al., 2018; Sunde, He, Hubbart, & Urban, 2017; Vörösmarty, Douglas, Green, & Revenga, 2005; Vörösmarty, Green, Salisbury, & Lammers, 2000). Water scarcity, the lack of fresh water resources to meet the standard water demand, is also likely to be a serious problem by the end of the 21st century in water management because of a growing demand for domestic, agricultural and industrial water use (Haddeland et al., 2014; Holland et al., 2015; Vörösmarty et al., 2000).

The Mediterranean climate is characterized by dry summers resulting from stable anticyclonic circulations and wet winters caused by mid-latitude frontal cyclones (Arnell & Gosling, 2013; Gampe, Nikulin, & Ludwig, 2016; Gao & Giorgi, 2008; Giorgi & Lionello, 2008; Hoerling et al., 2012; Peel, Finlayson, & McMahon, 2007; Samaniego et al., 2018). Studies of climate variability using global and regional climate models based on both observation data and various greenhouse gas emission pathways for the Mediterranean Basin suggest this area will be adversely affected by climate change in the future (T. Ozturk, Ceber, Türkeş, & Kurnaz, 2015; B. Sen, Topcu, Türkeş, Sen, & Warner, 2012; Stocker et al., 2013; Turp, Öztürk, Türkeş, & Kurnaz, 2014). Furthermore, the Mediterranean Basin is one of the most vulnerable regions in the world in terms of anthropogenic warming impacts on the hydrological cycle, being described as a “hot spot” for change (Giorgi, 2006). For instance, annual precipitation is likely to decrease across almost the entire region in the future (T. Ozturk et al., 2015). As a consequence of this decrease, Turkey, and especially coastal areas of the country adjacent to the Mediterranean, will face significant additional pressures on water resources (Aksoy, Unal, Alexandrov, Dakova, & Yoon, 2008; Fujihara, Tanaka, Watanabe, Nagano, & Kojiri, 2008; Onol, Semazzi, & F., 2009). In addition to coastal areas, a long-term decrease in future amounts of snowfall, surface runoff, and winter precipitation has been projected by Bozkurt and Sen (2013) for regions in the interior parts of Anatolia. When the long-term average annual and monthly total precipitation trends in Turkey are analysed a declining trend can be seen (Partal & Kahya, 2006). However, since 1980, there has been an increase in precipitation in the northern and eastern parts of the country, while a decrease has been observed in the centre, south and west (Türkeş et al., 2016). According to regional climate model results, long term decreases in daily precipitation are expected in western and southern regions of Turkey where Mediterranean climates dominate (T. Ozturk, Türkeş, & Kurnaz, 2011).

Global or Regional Climate Models (GCMs and RCMs) allow a quantitative exploration of potential changes in climate. Integrating GCM and RCM outputs with hydrological models is an important methodology to reveal the impact of climate change on hydrological processes as there are many non-linearities in catchment responses to rainfall and evaporation changes. This approach takes GCM or RGM outputs and uses this to force hydrological models in order to derive water balance components for watersheds such that the impacts of climate change on water resources can be investigated (Angelina, Gado Djibo, Seidou, Seidou Sanda, & Sittichok, 2015; Chattopadhyay & Jha, 2016; Ertürk et al., 2014; Fujihara et al., 2008; Stehr, Debels, Romero, & Alcayaga, 2008; Sunde et al., 2017; Zeng, Xia, She, Du, & Zhang, 2012). For example, Bucak et al. (2017) demonstrated the risk of drying of Beyşehir Lake due to climate change by using the SWAT hydrological model coupled with regional climate model outputs. However, outputs of General Circulation Models (GCMs) are often too spatially coarse to investigate hydrological impacts at many river basin scales. Therefore, GCM outputs are downscaled either dynamically or statistically using various methods (Chen, Xu, & Guo, 2012; Ertürk et al., 2014; Fowler, Blenkinsop, & Tebaldi, 2007; Maraun & Widmann, 2018; Sunde et al., 2017; Wilby & Wigley, 1997; Wood, Leung, Sridhar, & Lettenmaier, 2004). In this study, we have used 10-km high-resolution regional climate model outputs that have been dynamically downscaled from 50 km.

Reservoirs and dams are one of the main engineering management approaches to cope with droughts, floods and water scarcity issues (Gaupp, Hall, & Dadson, 2015; Vörösmarty et al., 2000). However, dams and reservoirs can have a serious negative impact on environmental, aquatic and fluvial systems (Graf, 1999, 2006; Magilligan & Nislow, 2005; Grill et al., 2019; Latrubesse et al., 2017). For example, one of the strong impacts of reservoirs is to create spatial fragmentation along fluvial systems (Graf, 1999; Grill et al., 2019). For instance, only 23% of rivers greater than 1000 km long flow the ocean without any obstacle (Grill et al., 2019). In addition to the spatial fragmentation of rivers, the natural flow characteristics of rivers associated with high and low flow hydrographs and their timing are influenced by the construction of water infrastructure. This can also affect the ecology and biodiversity of the riparian zone (Graff, 2006; Magilligan & Nislow, 2005; Poff, Olden, Merritt, & Pepin, 2007). However, these immense impacts of reservoirs and dams do not often outweigh the pressures and requirements for agricultural, industrial and domestic water supply and security (Destouni, Jaramillo, & Prieto, 2013; Haddeland et al., 2014). There are thus strong reasons only to construct the minimum number of reservoirs that are required given climate change and increasing demand. However, few studies to date have examined the impact of reservoirs on water resources and hydrological processes within catchments under different climate scenarios. The main objectives of this research are therefore:

1. to show the impact of reservoirs on water resources in a semi-arid catchment. In this context, two different scenarios, with the reservoir (RSV) and without the reservoir (WRSV), are presented by hydrological model that forced by climate model outputs.
2. to investigate the impact of long-term and seasonal climatic variations on water resources by evaluating future water availability using high-resolution regional climate model outputs under optimistic (RCP 4.5) and pessimistic (RCP 8.5) Representative Concentration Pathways (Van Vuuren et al., 2011).

2 | DATA AND METHODS

2.1 | Study area

The Susurluk basin, which is situated in the northwest part of Turkey (Figure 1(a)), covers an area of 23 779 km^2 and has elevation ranging between 2543 m (Uludağ Mountain) and 0 m m.s.l. (Figure 1(b)). Streams draining the basin include the Mustafakemalpaşa, Kocaçay, Nilüfer and Simav rivers, and in addition there are two large lakes: Uluabat and Manyas. The basin is predominately characterized by a

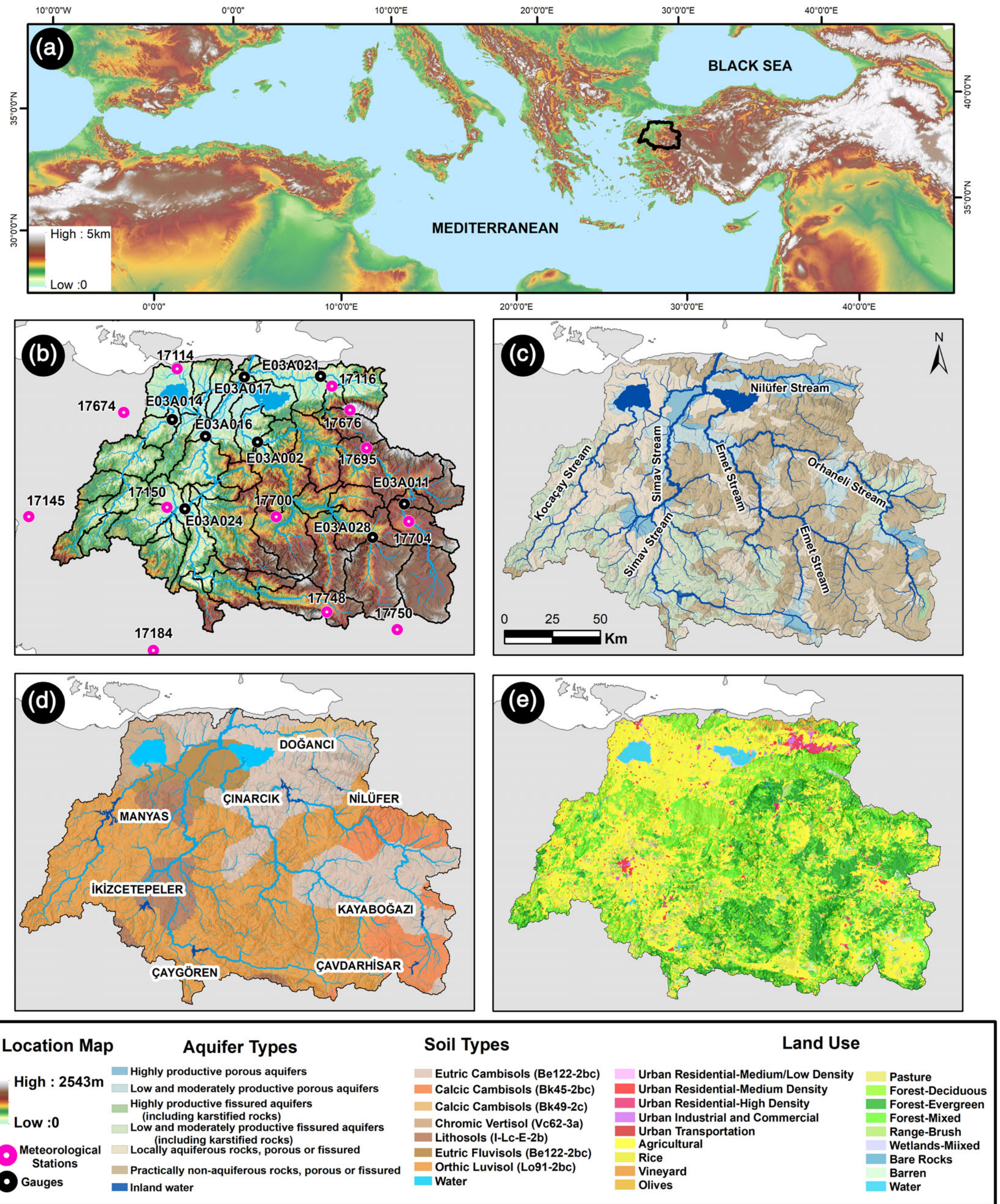

FIGURE 1 (a) Location map of the Susurluk basin in the Mediterranean Basin (b) Location of rainfall stations and gauges and Topographic map (c) Distribution of aquifer types (map was adopted by IHME1500 v11) (d) Distribution of soil types in the basin (e) Corine land-use map of the Susurluk Basin

Mediterranean macro climate (C) according to Köppen climate classification, with wet winters and dry summers. However, the Nilüfer sub-basin, where the Uludağ Mountain is located, is characterized by a mountainous climate (M. Z. Ozturk, Cetinkaya, & Aydin, 2017; Peel et al., 2007). The basin receives 570 mm average annual precipitation while the annual average runoff is 228 mm (Ayaz, 2010). This illustrates that almost half of rainfall turns to runoff in the basin. Figure S4 depicts the long-term monthly variation of rainfall and runoff with uncertainty bands, which was calculated with 5th and 95th percentile, for the 1983–2005 period. The highest values for rainfall and runoff are observed during winter months (DJF) in the Susurluk Basin, which are likely associated with mid-latitude frontal cyclones originating from the Atlantic and caused by polar air masses. Furthermore, the lowest runoff values are seen during summer (JJA) due to low precipitation and high evaporation (Akbas & Ozdemir, 2018) associated with high-pressure systems such as the Azores High and extension Monsoon Low (Barry & Chorley, 2009; Karaca, Deniz, & Tayanç, 2000; Tatli, Nüzhet, & Mentes, 2004). Peak values for runoff are observed in spring as a result of snow melt in upland areas.

The basin has a number of aquifers that are used to supply water resources. While the Bursa, Balıkesir, MustafaKemalpaşa and Simav plains have highly productive porous aquifers, other areas of the basin that drained by the Simav and Kocaçay rivers consist of low and moderately productive fissured aquifers and highly productive fissured aquifers, respectively (Figure 1(c)). In contrast, Orhaneli and Emet Stream watersheds have no viable aquifer resources.

A number of reservoirs already exist in the basin including Kayaboğazı (storage: 37.84 hm^3, construction date: 1987), Çavdarhisar (38.8 hm^3 1991), Selahattin Saygı-Doğancı (41.27 hm^3-1984), İkizcetepeler (157.29 hm^3, 1992), Çaygören (159.5 hm^3-1971), Manyas (423.39 hm^3, 2002) and Çınarcık (304.75 hm^3, 2003) which were constructed to supply water for irrigation, flood protection, domestic water and power generation (Figure 1(d)). There are also ongoing reservoir construction projects due to increasing demands for water (Koç, 2014; Yuksel, 2015). The prevailing land-use types in the basin are urban (476 km^2), agriculture (9997 km^2), and forest (10 876 km^2), and the basin is one of the most densely populated basins in Turkey (Figure 1(e)). Many big cities, such as Bursa, Balıkesir and Kütahya, lie within the borders of the basin and the total population was 3 201 773 at the 2017 census (General Directorate of Water Management [GDWM], 2018).

2.2 | General methodology

The main aim of this study is to simulate the Susurluk basin with and without reservoir scenarios, while simultaneously considering the impact of climate change, using the SWAT rainfall-runoff model developed by USDA Agriculture Research Service (ARS) (Arnold et al., 2012; Arnold, Srinivasan, Muttiah, & Williams, 1998). SWAT is a physically-based model, which means that it requires physical data such as soil, vegetation, weather data and topography, and has been shown to be capable of simulating long-term changes in watersheds (Neitsch, Arnold, Kiniry, & Williams, 2011). The model divides the basin into many sub-basins and overlays slope, land-use and soil in order to generate HRU (Hydrological Response Unit) which enable the model to calculate physical processes in each unique unit.

Simulations of the hydrological cycle in SWAT are based on the water balance equation as follows:

$$SW_t = SW_0 + \sum_{i=1}^{t}\left(R_{\text{day}} - Q_{\text{surf}} - E_a - w_{\text{seep}} - Q_{gw}\right), \tag{1}$$

where, SW_t is final soil water content (mm H_2O), SW_0 is initial soil water content (mm H_2O), t is the times (days), R_{day} is the amount of precipitation on day i (mm H_2O), Q_{surf} is the amount of surface runoff on day i (mm H_2O), E_a is the amount of evaporation on day i (mm H_2O), w_{seep} is the amount of water entering the vadose zone from soil profile on day i (mm H_2O), Q_{gw} is the amount of return flow on day i.

The model requires four key data sets; A Digital Elevation Model, land use, soil and observed meteorological and hydrological data. The specific data sources used in this application were as follows:

Digital elevation model

SRTM (Shuttle Radar Topography Mission) digital elevation model (90 m resolution) which is hydrologically conditioned by HydroSHEDS (Hydrological data and maps based on Shuttle Elevation Derivatives at multiple Scales) was used in this study (Lehner, Verdin, & Jarvis, 2008). A 15 000 ha value was used as a threshold to obtain river networks and 58 sub-basins were extracted in the basin (Figure 1(a)).

Land use

In this study, the Corine Land use-Landcover database was employed and converted to the SWAT land use classification (Figure 1(d)).

Soil database

Soil data was obtained from the 1:5 000 000 scaled Harmonized World Soil Database (1 km resolution, http://webarchive.iiasa.ac.at/Research/LUC/External-World-soil-database/HTML/). Orthic Luvisols soils (47.5%, percentage of soil cover) cover almost half of the basin, and Eutric Cambisols (27.6%) are the other dominant soil type. Other soil types, such as Calcic Cambisols, Lithosols, Eutric Fluvisols and Chromic Vertisols, cover 24.8% of the basin (Figure 1(c)).

Meteorological and hydrological database

Daily and monthly meteorological data from 1982 to 2005 were obtained from the Turkish State Meteorological Service (TSMS). The daily data comprises time series for precipitation (mm), relative humidity (%), wind speed (m/s), solar radiation (MJ/m^2) and minimum and maximum temperature (°C), and were obtained by the meteorological stations at Bandırma (WMO code: 17114), Bursa (17116), Edremit (17145), Balıkesir (17150), Akhisar (17184), Gönen (17674), Uludağ (17676), Keles (17695), Dursunbey (17700), Tavşanlı (17704), Simav (17748) and Gediz (17750) (see Figure 1(b)). Long-term monthly weather data from TSMS was also used to impute missing values in the daily time series and generate climatic data. A hydrological database from river gauges was obtained from the Turkish Hydraulic Service (DSI) for calibration of the SWAT rainfall-runoff model. Data from gauges at Nilüfer Çayı-Geçitköy (Station code: E03A021), Kocadere-Akçasusurluk (E03A017), Kocaçay-Kayaca (E03A014), Mustafa Kemalpaşa Çayı-Döllük (E03A002), Simav Çayı-Yahyaköy (E03A016), Atnos Çayı-Balıklı (E03A024), Emet Çayı-Dereli (E03A028), and Orhaneli Çayı-Küçükilet (E03A011) (Figure 1(b)) were selected as these have records covering the same period as the meteorological data. Figure 1(a) shows the location of meteorological stations and gauges.

The methodology of this study is given in Figure 2. First, physical variables such as land cover, soil and slope were used to generate HRUs. Initial parameter estimates from available data for SWAT require calibration to refine simulations and predictive skill. The SWAT Calibration and Analysis Program (SWAT-CUP) was used to calibrate the model using observed monthly river discharge values. Important parameters that are sensitive were selected and model was calibrated based on its ability to replicate the observations. Next, outputs from the global climate model MPI-ESM-MR were dynamically downscaled from 50 to 10 km grid resolution using the RegCM4.4 regional climate model. Outputs representing the RCP 4.5 and RCP 8.5 pathways were selected and used to force the calibrated SWAT model. Simulations were performed for mid-century (2020–2049) and late-century (2070–2099) conditions. Before running climate model data outputs through the rainfall-runoff model, bias corrections for precipitation and temperature were utilized to eliminate these effects (see Appendix S1). The last process of the analysis is running the model with different reservoir scenarios and climate pathways as follows:

- Reservoir (RSV): Simulations are executed representing current reservoir conditions in the basin.
- Without Reservoir (WRSV): Simulations are executed by assuming that there are no reservoirs in the basin.
- RCP 4.5: This is an optimistic pathway for combating climate change. In this pathway, it is projected that CO_2 concentration will be 487 ppm in the middle of the century and 538 ppm by 2100. It is estimated that radiative forcing will be 4.5 W/m^2 by the end of this century (Clarke et al., 2007; Meinshausen et al., 2011; Smith & Wigley, 2006; Van Vuuren et al., 2011; Wise et al., 2009).
- RCP 8.5: This is the most pessimistic pathway used in current climate projections and represents a "business as usual" world. In RCP 8.5 it is estimated that CO_2 concentration will be 541 ppm by 2050 and 936 ppm by 2100. It is estimated that radiative forcing will be 8.5 W/m^2 by the end of this century (Meinshausen et al., 2011; Riahi, Grübler, & Nakicenovic, 2007; Van Vuuren et al., 2011).

Thus, the impact of reservoirs under a changing climate and their impact on hydrological system (e.g., fluxes) within the basin can be revealed. In SWAT, we have selected outflow-target-release scenario (IRESCO = 2) for reservoir release simulation. In addition, the Falkenmark (1989) for water scarcity was used to quantify, differentiate and compare the impact of reservoir scenarios and climate pathways. This indicator allocates the water per person by taking water from rivers into account (see below). Finally, water resources were compared to differentiate the impact of climate change and reservoir scenarios (Figure 2-Third process). In order to understand water availability under different climate scenarios and time scales, water resources of whole Susurluk Basin have been calculated as blue water (deep aquifer recharge + water yield), green water storage (soil moisture), green water flow (evapotranspiration) instead of using many single parameters such as surface runoff and groundwater.

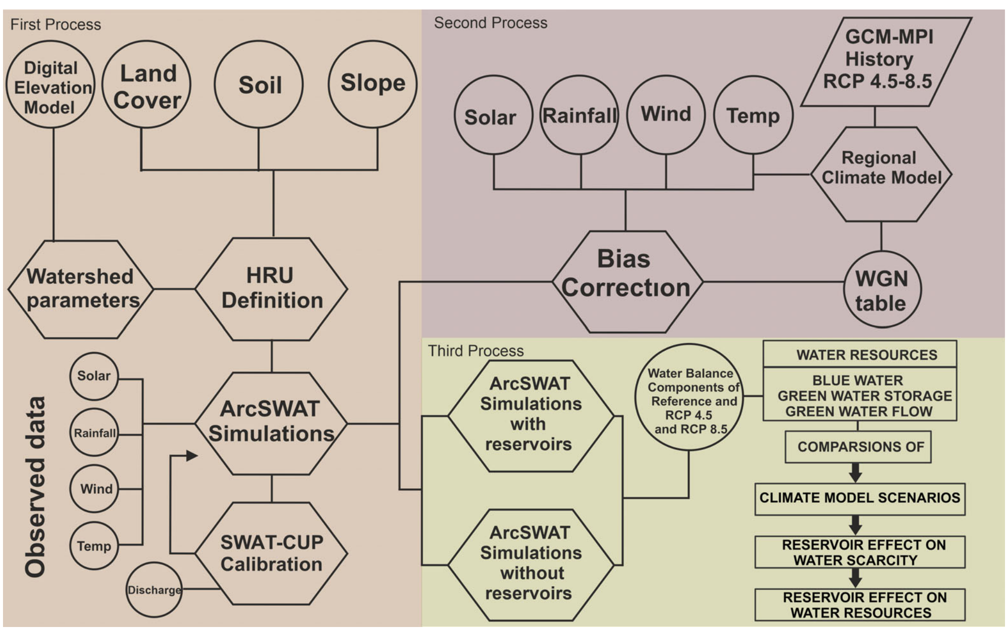

FIGURE 2 Flowchart of the study. The first process illustrates the settings of the rainfall-runoff model. How data are obtained from the regional climate model was explained in the second process. The third process demonstrates the comparison of interested parameters based on different reservoir scenarios and climate pathways

2.2.1 | HRU, parameterization, calibration and performance tests for SWAT model

HRUs were determined by overlaying soil, land use and slope data. The value of the soil was chosen as 0% for the land use, 0% for the slope and 0% for the soil. Thus, 3500 HRU values were obtained in the basin. The Penman-Monteith method was used to calculate evaporation and transpiration (Monteith, 1965) and the Soil Conservation Service (SCS) Curve Number method was used for surface runoff estimation in the sub-basins (SCS, 1956, 1964, 1971, 1985, 1993).

The SWAT model was calibrated by using the Soil and Water Assessment Tool Calibration and Analysis Program (SWAT-CUP) with the observed data (Abbaspour, 2013). Sequential Uncertainty Fitting (SUFI-2) was utilized as the calibration algorithm with uncertainty levels of 95 PPU. The SUFI-2 method has two options: "replace" is the option that changes original parameter values in ranges, while "relative" uses artificial ranges instead of the original parameter ranges (see Table 1). Eight different and sensitive parameters have been selected based on the study of Abbaspour et al. (2015) in order to reduce the error in simulations. Three hundred iterations of the SUFI-2 algorithm were executed via the Nash–Sutcliffe efficiency (NSE) criterion and the best values of calibrated parameters (Table 1) were obtained according to this criterion. All analyses for both reference and future scenarios were conducted based on optimal calibrated parameter values. The other evaluation tests below were used as indicators or evaluation tests of the coherence of the model and observed values.

The Nash–Sutcliffe efficiency (NSE) (Krause, Boyle, & Bäse, 2005; Nash & Sutcliffe, 1970) was employed to evaluate simulation results at gauges (Figure 1(a)). The NSE coefficient can be expressed as:

$$\mathrm{NSE} = 1 - \sum_{i=1}^{n} \frac{(Q_i - P_i)^2}{(Q_i - \bar{Q})^2}, \tag{2}$$

where $\bar{Q}$ is the mean of observed discharges, and Q is simulated discharge. P_i is observed discharge at time t. The Nash-Sutcliffe efficiency (NSE) compares the residual variance of simulation with the variance of the observations. (Nash & Sutcliffe, 1970). Nash-Sutcliffe efficiencies range from $-\infty$ to 1. NSE = 1, corresponds to a perfect match between simulated and observed data. NSE = 0 indicates that the model predictions are as accurate as the mean of the observed data, $-\infty < \mathrm{NSE} < 0$, indicates that the observed mean is a better predictor of the observations than the model. Moriasi et al. (2007) explain that an NSE greater than 0.5 is satisfactory for simulation results.

The second test is the Percent BIAS (Gupta, Sorooshian, & Yapo, 1999). The PBIAS coefficient can be expressed as:

$$\mathrm{PBIAS} = \left[\frac{\sum_{i=1}^{n} \left(Y_i^{\mathrm{Obs}} - Y_i^{\mathrm{Sim}} \right) * 100}{\sum_{i=1}^{n} \left(Y_i^{\mathrm{Obs}} \right)} \right], \tag{3}$$

where Y_i^{Obs} observed discharge at time t, Y_i^{Sim} simulated discharge at time t. PBIAS is based on the percentage difference of the simulation from the observations. Zero is an optimal number that shows the reliability of the model for simulation. The number $\pm 15 < \mathrm{PBIAS} < \pm 25$ is typically considered satisfactory for PBIAS (Moriasi et al., 2007).

The last test is linear regression, which is used in extensively hydrological modelling studies. The regression coefficient can be expressed as:

$$R^2 = \left(\frac{\sum_{i=1}^{n} (Q_i - \bar{Q}) - (P_i - \bar{P})}{\sqrt{\sum_{i=1}^{n} (Q_i - \bar{Q})^2} - \sqrt{\sum_{i=1}^{n} (P_i - \bar{P})}} \right)^2, \tag{4}$$

where R^2 is the coefficient of determination, Q is observed, and P is simulated runoff from the simulation. Regression coefficients indicate

TABLE 1 Calibrated parameters of the model gathered from SWAT-CUP for the Susurluk Basin

Name of parameters	Definition of parameters	Initial ranges	Ultimate ranges	Best value	*t* value	*p* value
r_CN2.mgt	SCS curve number values for moisture condition II	−0.2 to 0.2	−0.31 to 0.03	−0.14	−14.06	1.24×10^{-34}
v_ALPHA_BF.gw	Baseflow alpha factor (1/days)	0–1	0.27–0.81	0.54	1.65	0.10
v_GW_DELAY.gw	Groundwater delay time (days)	30–450	−53.04 to 282.44	114.70	−0.87	0.39
v_GWQMN.gw	Threshold depth of water in the shallow aquifer for return flow (mm H_2O)	0–5000	−2063.57 to 2646.90	291.67	1.36	0.17
v_REVAPMN.gw	Threshold depth of water in the shallow aquifer for revap (mm H_2O)	0–50	9.11–36.39	22.75	−0.27	0.79
v_GW_REVAP.gw	Groundwater revap coefficient	0.02–0.2	−0.01 to 0.13	0.06	3.09	2.22×10^{-03}
v_ESCO.hru	Soil evaporation compensation factor	0–1	−0.21 to 0.60	0.19	−2.37	0.02
r_SOL_AWC.sol	Soil available water storage capacity(mm H_2O/mm soil)	−0.2 to 0.2	−0.35 to 0.02	−0.16	2.29	0.02

Note: r refers to relative changes for given ranges while v refers to replace changes.

the dispersion between observed and modelled time series. The numbers of the coefficient of determination range from 0 to 1. While $R^2 = 0$ describes randomness between observed and modelled, 1 is an optimal value at which dispersion is low.

2.3 | Water scarcity indicator

The Falkenmark indicator (Falkenmark, 1989) was employed to understand the availability of water in the study area and was chosen because of its relative simplicity. The indicator evaluates the amount of water per capita population and can be expressed as:

$$FI\,(m^3/cap/yr) = \sum_{Day=1}^{365} m^3/\text{Population}, \tag{5}$$

where, m^3 is daily water amount which is summed for the year. The population is the total who live in the analysis area. Water stress can be categorized based on fraction water for per capita usage. 1700 m^3 per capita is a key threshold for this index. If annual water availability per capita is below 1700 m^3 water stress begins. Water availability between 1000 and 500 m^3 is an indicator of scarcity and below 500 m^3 represents absolute scarcity for the affected area (Falkenmark, 1989). Data for the population was obtained from The Global Population Projection Grids Based on Shared Socioeconomic Pathways (SSPs) dataset (Jones & O'Neill, 2016, 2017) which has a resolution of 7.5 arc-minutes. Projected population data for the Susurluk Basin was extracted for 2010–2100 (-Figure S6). Each SSP pathway represents different trends, which indicate different socio-economic futures for each country. We employed all five SSP scenarios in this study to cover the full spread of possible scenarios. Observed population data for 1980–2000 was obtained from the TURKSTAT (Turkish Statistical Institute, 2018) in order to compare the reference period with respect to the future period for the whole basin.

3 | RESULT AND DISCUSSION

3.1 | Calibration results in Susurluk Basin

Table 1 shows the parameters, descriptions, ranges and sensitivity of parameters. t and p values refer to the sensitivity of parameters obtained from multiple regression analysis. Larger values of t and smaller values of p (significance level) indicate that parameters are more sensitive in the model. The SCS Curve Number Values for Moisture Condition II (CN2) is the most sensitive parameter, followed by the Groundwater REVAP coefficient (GW_REVAP), Soil Evaporation Compensation factor (ESCO) and Soil Available Water Storage Capacity (SOL_AWC). Modelled runoff is also sensitive to other parameters, but not to the same extent as the parameters mentioned above.

Observed discharge values at the gauges in the basin were compared with modelled runoff values through the model performance test in Figure 3 based on virtual reservoir scenarios. Figure 3 shows that the simulated time series for the Simav and Kocaçay rivers (Figure 1(b), gauges E0A014, E0A016 and E0A024) cannot match the peak flow of observed runoff; even though it manages to track trends or oscillations in the observed runoff. Monthly error plots illustrate that this underestimation is higher in the winter season (Figure 3) and this may be a consequence of the groundwater in these areas. Because this underestimation occurs in areas that contain highly productive fissured aquifers, this may mean that karstic processes are important here (Figure 1(c)). Nevertheless, performance test results are generally sufficient for the science objectives of the paper. In the Nilüfer and Emet sub-basins, where gauges with E03A021 and E03A028 codes are located, the model cannot simulate some peak flood events observed in the spring season, however the evaluation test results are sufficient according to the guidelines of Moriasi et al. (2007). This circumstance might be a consequence of a higher topography in which precipitation falls as snow in winter and the timing of snowmelt controls the flood peaks in the basin. It is also important to account for possible errors in the observed discharge data (e.g., Coxon et al., 2015) in drawing conclusions about the model performance. In general, performance testing of the model shows sufficient scores (Figure 3) in terms of evaluation criteria of Moriasi et al. (2007) except for two stations. However, this two stations have no great influence of test scores at outlet. For example, in Figure 3, gauge E03A017 represents almost whole the basin excluding Nilüfer sub-basin. The performance test values for gauge E03A017 are 0.63 for NSE, 0.15 for PBIAS, and 0.68 for R2, respectively. Therefore, it can be said that the skill of the calibrated model is sufficient to accomplish the aims of this study.

3.2 | Water availability under climate change pathways

We evaluated the impact of climate scenarios on water resources along with reservoir scenario (RSV) in order to reflect the actual situation in the basin. A boxplot of all water resources was drawn to distinguish the gradient of all RCP's. A nonparametric test of Mann–Whitney U or Wilcoxon rank-sum tests (Lehmann & D'Abrera, 1975) were utilized in order to compare and contrast the statistically significant change in monthly water resources components (precipitation, blue, green water storage and green water flow) for future periods under the RCP 4.5 and RCP 8.5 climate model pathways with respect to the reference period (Figure 4).

Figure 4 illustrates that there is a statistically significant decrease for all water resource components in the future periods of RCP4.5 and RCP8.5 with respect to the reference period except for green water flow. Decreases in future precipitation were observed for all RCPs except for the RCP4.5 late century (2070–2099) pathway. The simulation results also indicate that there will also be a statistically significant decrease for blue water in the future for both RCP 4.5 and RCP 8.5 in comparison with the reference period. The intensity of this decrease will be more severe than other water resources according to the significance level. Also, the median, 25th and 75th percentiles of blue water will likely decrease more than the other resource

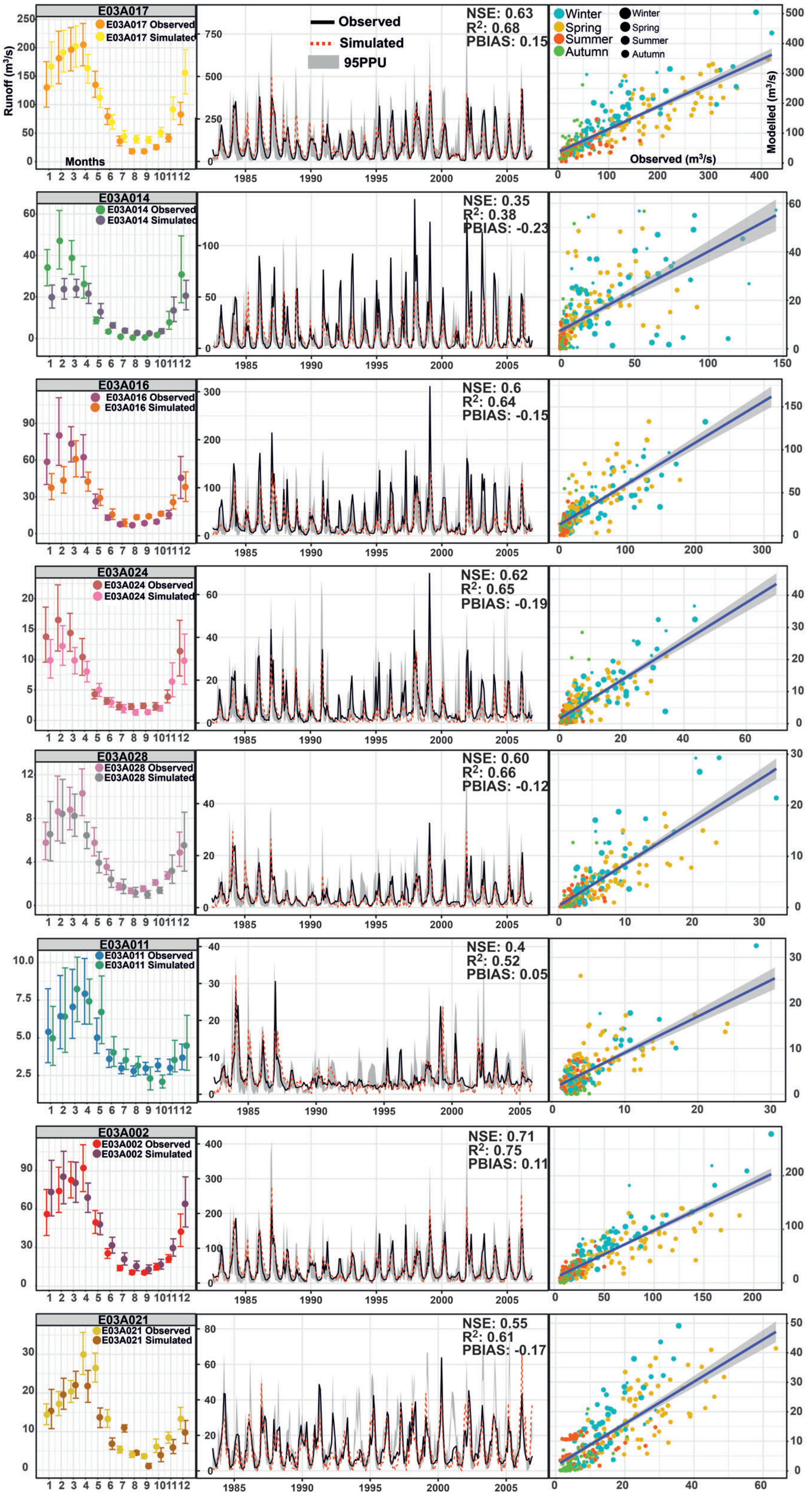

FIGURE 3 Comparison of monthly simulated and observed runoff in the Susurluk Basin. The left side of the graphs indicates a monthly error plot. Middle graphs are time series of observed and simulated runoff with 95% prediction uncertainty (95PPU). The right side of graphs demonstrate scatter of observed vs simulated runoff at the seasonal time scale

components when comparing the reference period with late century pathways. Outliers (extremes) of boxplots will increase on the contrary of median and percentiles. Similar to blue water, a statistically significant decrease was seen for green water storage for both RCPs with respect to the reference period. On the other hand, there is no statistically significant decrease or increase in green water flow for the future of RCP 4.5 and RCP 8.5 except for RCP4.5 mid-century (2020–2049). Although a statistically significant change in green water flow was not detected, the 25th and 75th percentiles of green water flow do decrease in the future. Figure 4 also shows a remarkable decrease for all water resources for the RCP8.5 scenario by late century (2070–2099). The variability of climate model pathways in terms of increasing and decreasing water resources is as expected according to radiative forcing scenarios (Stocker et al., 2013; Van Vuuren et al., 2011). Besides, Gorguner, Kavvas, and Ishida (2019) have studied the Gediz basin, which is close to the Susurluk Basin, in order to determine the impact of climate change on streamflow using a different kind of model and ensembles for RCP4.5 and RCP8.5. This study showed that there will be a decrease in streamflow according to the ensemble of all projections similar to that expected for blue water (freshwater) in this study.

Kernel density plots, which is non-parametric method for estimating the probability density function of random variable, were drawn in order to understand possible future shifts in water resources at seasonal scales. Figure S5 shows that there is noticeable dispersion in all parameters and all seasons, even though the magnitudes or amplitudes may be different. For all parameters excluding green water flow, the densities under RCP4.5 and RCP8.5 have moved to the left side of the reference period in entire seasons. Similarly, peak densities of RCPs have shifted either upward or downward from the reference period. Peak of all densities of all parameters are outstanding in the summer season in which the values of all water resources, which is spread around the tail, are low because of drought season. Both the peaks and tails of the density plot of RCP4.5 and RCP8.5 for precipitation in winter follow the density of the reference period. Densities of mid-late century RCP4.5 and RCP8.5 for spring have shifted to the left of the reference period. In summer, precipitation decreases in all RCPs for the future in comparison with the reference period; however, the amplitude of peaks between 0 and 25 mm have increased, especially in the late century RCP8.5 scenario. Similar to winter, RCP 4.5 and RCP 8.5 autumn precipitation density curves fluctuate around the reference period curve, yet the late century of RCP4.5 (2070–2099) has shifted from the right side of the reference. The amplitude of peak and tales of blue water densities for all RCPs have shifted to the left side of the reference period. In addition, peak values have slightly increased when compared to the reference period. Nevertheless, winter, summer and spring seasons are more vulnerable than autumn in terms of change. The conditions that are seen for blue water is the same for green water storage as well. However, the winter season of the green water flow has the opposite character than other parameters that before explained. Outside of other seasons of the green water flow, RCPs of winter tend to move the right side of the reference period. Generally, autumn is more stable in terms of shifting and changing of curves around the reference period. The same changes, in particular for precipitation, around the basin, have been detected by many researchers (Demircan, Gürkan, Eskioğlu, Arabacı, & Coşkun, 2017; Giorgi & Lionello, 2008; Lelieveld et al., 2012; Onol et al., 2009; T. Ozturk et al., 2015; Turp et al., 2014). It is seen that climate change has a strong impact on water resources by changing the water amount. However, it is not well understood and documented how the reservoir is changing the available water in basins. Therefore, scenarios of the reservoir with climate impact pathways for water resources have been compared in the next section.

3.3 | Reservoir effect on water resources

The Falkenmark indicator (Falkenmark, 1989) was employed based upon climate model pathways (RCPs), observed (TURKSTAT) and

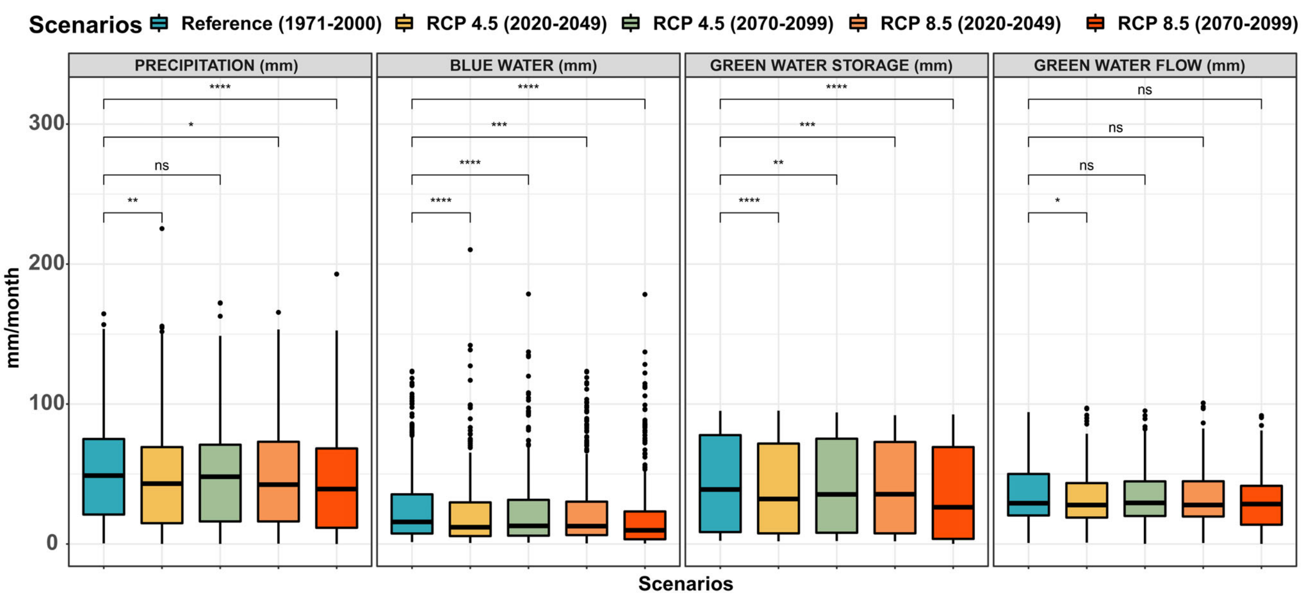

FIGURE 4 Boxplot comparisons of water resources under different scenario results (The stars at top of facet indicate the significance values of Mann–Whitney *U* test; ns: $p > 0.05$, *: $p < =0.05$, **: $p < =0.01$, ***: $p < =0.001$, ****: $p < =0.0001$)

socio-economic population scenarios (SSPs) in order to depict the effect of the reservoir scenarios and climate change pathways on blue water scarcity. Bar graphs were created by dividing the population in each decade by average decadal runoff from the basin outlet (Figure 5). For this, the hydrological model was employed with two reservoir scenarios (RSV, WRSV) to illustrate the water that is needed to cope with scarcity based upon the Falkenmark indicator. The threshold that indicates blue water scarcity was added to the bar plot as a dashed line and a pie chart was constructed to show the proportions of water in runoff and water stored in the reservoirs.

The results demonstrate the different combinations of climate, population and reservoir scenarios. As seen in Figure 5, the quantity of water per capita with reservoirs (RSV) is less than the without reservoirs (WRSV) scenario. Water for per capita is especially abundant during the reference period because of a small population (Figure 5(a) and Figure S6). SSP3, which is the worst-case scenario for the population scenario, shows that water for per capita is going to be down almost 500 m^3 by 2100 under the RSV scenario. However, SSP5 and SSP1 scenarios, which limits population growth, demonstrates that water per capita does not cross the dashed line in either of the RSV or WRSV scenarios. In general, Figure 5 illustrates that all population scenarios will likely experience blue water scarcity due to the lack of available water and an increase of population up to 2100. Furthermore, the difference of water scarcity among reservoirs scenarios is

FIGURE 5 (a) Falkenmark indicator results based on climate and population scenarios (dashed lines indicate no scarcity or water stress), (b) ratio of water (m^3) in runoff and reservoirs

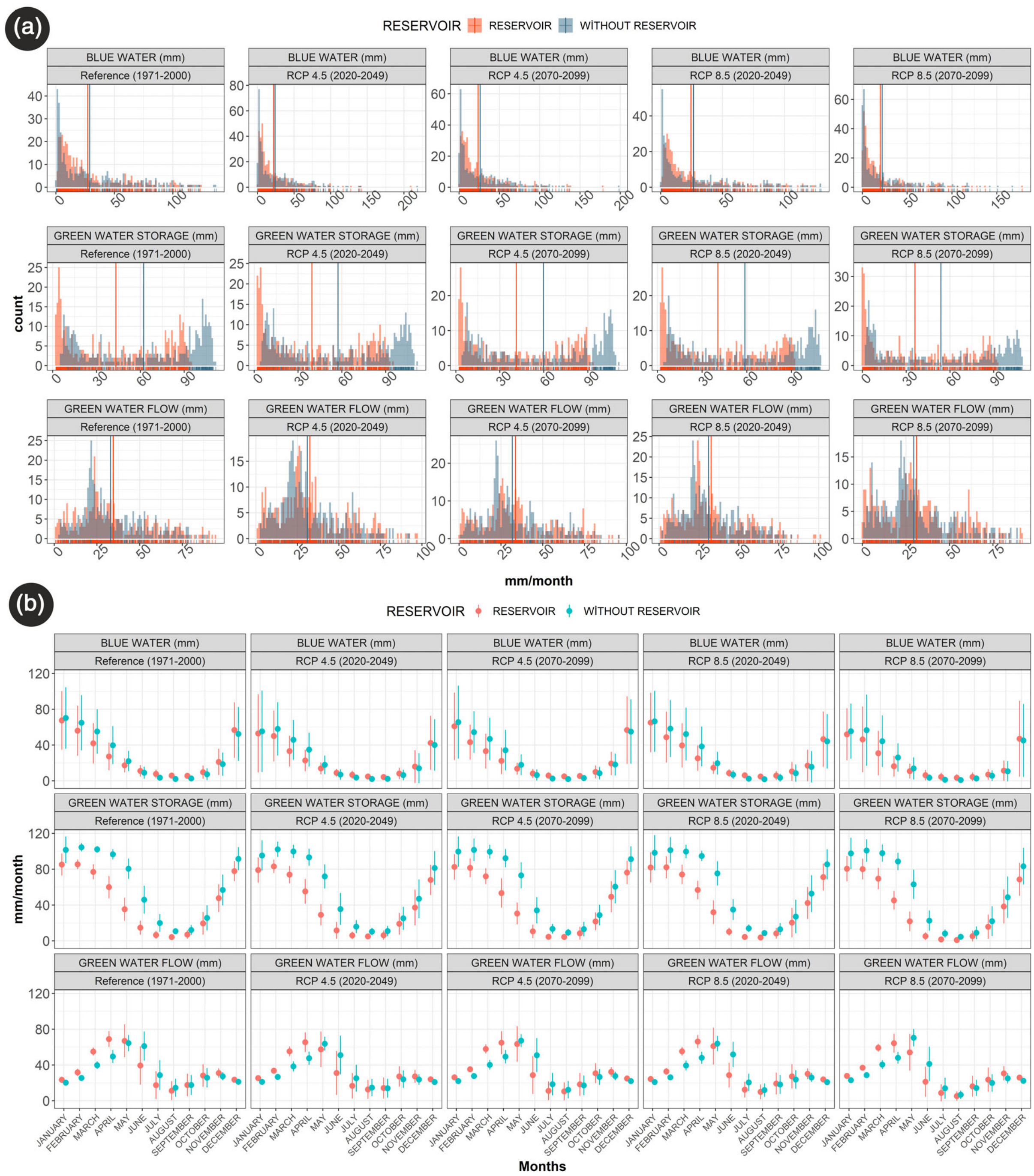

FIGURE 6 (a) Histogram distributions of water resources of Susurluk Basin (lines in the histograms are mean values) (b) Error plots of water resources of Susurluk Basin based on the reservoir and climate scenarios

relatively low. Since the target-release scenario (IRESCO = 2) has been chosen, required water for river can be released when and after accumulation. However, the Falkenmark indicator focuses on the amount of water that is accessible from river courses and neglects the water accumulated in reservoirs.

Hence, in this study, the water accumulated in the reservoirs in the Susurluk Basin was taken into consideration for water scarcity assessment. Figure 5(b) illustrates that the ratio of water from runoff for three decades in the reference period is higher than the future periods owing to the reservoirs that have been built during this period (Çaygören (159.5 hm^3-1971), Kayaboğazı (37.84 hm^3-1987), Selahattin Saygı-Doğancı (41.27 hm^3-1984), İkizcetepeler (157.29 hm^3-1992), Çavdarhisar (38.8 hm^3-1991)). After the reference period, the proportion of water from runoff is seen to decline compared with water in reservoir. This illustrates that the proportion water in reservoir and runoff change with the date of water infrastructures. For instance, after reference period, such big reservoirs as Manyas (423.39 hm^3-2002) and Çınarcık (304.75 hm^3-2003) were built for irrigation, flood protection and drinking water and then the proportion of waters in pie chart stay in same because there is no any construction in inventory of SWAT. According to the Falkenmark indicator, the Susurluk Basin will suffer from water scarcity in the future because runoff does not meet the water demand of the population. However, measures such as building reservoirs indicate that focusing only on blue water scarcity from runoff can be misleading for basins. In particular, Figure 5(b) shows that future scarcity can be countered with reservoir construction (Figure 5(b)). For that reason, in classical water management, reservoirs can be seen as an effective way to handle water scarcity and drought according to the results of this study. This perception drives society to put pressure on decision-makers to build reservoirs in order to protect populations from economic damage, yet according to Di Baldassarre et al. (2018) as a result society can become more fragile due to overdependence on such water infrastructure as they may prevent the adoption of other, more sustainable measures such as water conservation.

Figure 6 demonstrates the impact of reservoirs on water resources. As explained previously, blue water will decrease in the future under both RCPs, but the RSV scenario intensifies the magnitude of this decrease as well (Figure 5(a)). Figure 6(a) illustrates that the quantity of blue water below 25 mm in RSV is higher than the WRSV scenario. However, this condition reverses for values higher than 25 mm and blue water in WRSV increases its frequency for higher values. The decrease in blue water is not similar in all months. Figure 6(b) shows that the gap of error plots between the RSV and WRSV scenarios is higher in the February–May period (FMAM) for blue water under both RCPs. The gaps between RSV and WRSV are at a minimum in the June–December period (JJASOND) and even blue water values for the RSV scenario are higher than in the WRSV scenario in some months. This circumstance indicates that the both RSV and WRSV scenario does not make any change in amount the blue water in summer and autumn while it does make change in February and spring (MAY) for both reservoir scenarios. Although the gap between both reservoir scenarios in terms of blue water seems similar for both climate pathways, the quantity of water will decrease in all RCPs with respect to the reference period. According to RCP 4.5, blue water will decrease by mid-century and it will slightly increase in late-century, but it will not be higher than the reference period. For RCP 8.5, the blue water from mid-century to late-century will gradually decrease when compared to reference period.

Differences between reservoir scenarios in terms of green water storage are more remarkable than blue water. Figure 6(a) shows that green water storage for the RSV scenario has shifted to the lowest values with respect to WRSV. From a seasonal perspective, gaps between reservoir scenarios are salient in all months. Nevertheless, July, August and September are the months in which gaps between scenarios are at a minimum (Figure 6(b)). Climate change pathways for green water storage are similar to those for blue water. This illustrates that green water storage will be the most impacted water resource after the construction of reservoirs. Since green water storage is the most crucial water resource in order to supply water for food production (Rockström et al., 2009), a negative impact on green water storage may pose a risk for this activity. The main function of the six reservoirs in the basin is for irrigation, and other functions, such as flood protection, power generation and domestic water use, are secondary. Although building a reservoir can be seen as an effective way to meet agricultural irrigation demands, it creates a dilemma by reducing green water storage. In addition to the decrease in water resources, the RSV scenario also causes water losses by increasing the quantity of green water flow (Figure 6). Both histogram and error plots illustrate that green water flow will increase in the RSV scenario relative to WRSV. Moreover, Figure 6(b) shows that this increase will not be similar for all months, potentially due to water usage by vegetation. Water storage in open reservoirs can accelerate fluxes to the atmosphere through evaporation. Consequently, reservoirs can have a substantial impact on water resources by changing the amount of water fluxes, but climate change also intensifies the variability of water resources.

4 | CONCLUSION

This study depicts the combined and differentiated impact of climate change pathways and reservoir scenarios for a large Mediterranean basin using the SWAT rainfall-runoff model and downscaled climate scenarios. Climate change in the Susurluk basin will likely change the amount of future water resources, with decreases for precipitation, blue water and green water storage and increases for green water flow. It can obviously be said that climate change exacerbates the vulnerability of the basin by intensifying the variability of water resources.

Blue water scarcity for the Susurluk will likely be experienced in terms of reducing water per capita until 2100 for the basin according to the Falkenmark indicator. In particular, the population and climate model pathways illustrate that the basin will experience scarcity of blue water with below 1700 m^3 per capita for decadal changes. Nonetheless, the Falkenmark indicator only considers runoff from the river to quantify the scarcity of water in the basin. By contrast, the quantity of accumulated water in reservoirs is almost 100 times higher than water in streamflow. Hence, it can be seen as useful to build a reservoir for many purposes at first glance. However, the reservoir can cause drought and scarcity by accumulating water that would otherwise recharge river courses, aquifers, and soils. For that reason, the role of reservoirs in classical water management to address drought and scarcity problems brings a dilemma for socio-hydrological systems because of this disruption of the natural hydrological cycle. Stored water in reservoirs is mostly used to recharge green water storage for agricultural purposes. However, reservoirs can cause a decrease in green water storage as well. Therefore, the cost–benefit ratio can bring a dilemma before constructing a reservoir. Whereas, Falkenmark (2013) expresses that many places like semi-arid or arid regions, which cover almost the entire Mediterranean basin, have to protect green water storage because water consumption is higher than blue water during the growing season of crops in order to overcome drought and scarcity problem. For that reason, Rockström et al. (2009) suggest that green water storage has to be used efficiently with blue water, especially for agricultural purposes. Di Baldassarre et al. (2018) have questioned the emphasis on building water infrastructure in terms of the feedback mechanism of the supply–demand cycle and reservoir effect. They have concluded that many feedback mechanisms of social factors worsen water shortages since the high reliance on this source. In addition to measures to alleviate drought and water scarcity, economic growth plans bring a further dilemma for socio-hydrological systems because every country has a right to combat poverty and supply energy for their citizens. Hence, due to the pressure of increasing population, and consequent demands on water for energy, flood protection and economic growth plans (Koç, 2014), there will always be a requirement for new reservoirs for these purposes. Therefore, it would be important to underline that benefits deriving by the construction of reservoirs are always submitted to a correct management of the reservoir itself.

Finally, this study demonstrates that reservoirs can change the quantity of fluxes within watersheds. Therefore, it will also be valuable to consider the presence of reservoirs in hydrological modelling of watersheds in order to reduce the uncertainty of models and have more realistic values of water balance parameters.

ACKNOWLEDGEMENTS

This study was funded by TUBITAK-Scientific and Technological Research Council of Turkey with 2214-A Program and Scientific Research Program of Istanbul Üniversitesi-BAP (Project No: 57515, 39111 and 38985). Freer was partly funded for his time by the Global Water Futures program, University of Saskatchewan. Paul Bates is supported by a Royal Society Wolfson Research Merit award. We also would like to thank M.L. Kurnaz who is head of the Center for Climate Change and Policy Studies, Boğaziçi University for sharing high-resolution climate model data. We thank anonymous referees for their constructive and helpful comments on an earlier version of this paper.

DATA AVAILABILITY STATEMENT

The data that support the findings of this study are available from the corresponding author upon reasonable request.

ORCID

Abdullah Akbas https://orcid.org/0000-0003-2024-0565
Jim Freer https://orcid.org/0000-0001-6388-7890
Hasan Ozdemir https://orcid.org/0000-0001-8885-9298
Paul D. Bates https://orcid.org/0000-0001-9192-9963
M. Tufan Turp https://orcid.org/0000-0002-3980-2153

REFERENCES

Abbaspour, K. C. (2013). SWAT-CUP 2012. SWAT Calibration and uncertainty program—A user manual.

Abbaspour, K. C., Rouholahnejad, E., Vaghefi, S., Srinivasan, R., Yang, H., & Kløve, B. (2015). A continental-scale hydrology and water quality model for Europe: Calibration and uncertainty of a high-resolution large-scale SWAT model. *Journal of Hydrology*, *524*, 733–752.

Akbas, A., & Ozdemir, H. (2018). Marmara Denizi havzasının hidroklimatolojik dinamiklerinin belirlenmesi. *Türk Coğrafya Dergisi*, *70*, 123–131 (In Turkish).

Aksoy, H., Unal, N. E., Alexandrov, V., Dakova, S., & Yoon, J. (2008). Hydrometeorological analysis of northwestern Turkey with links to climate change. *International Journal of Climatology: A Journal of the Royal Meteorological Society*, *28*(8), 1047–1060.

Alfieri, L., Burek, P., Feyen, L., & Forzieri, G. (2015). Global warming increases the frequency of river floods in Europe. *Hydrology and Earth System Sciences*, *19*(5), 2247–2260.

Angelina, A., Gado Djibo, A., Seidou, O., Seidou Sanda, I., & Sittichok, K. (2015). Changes to flow regime on The Niger River at Koulikoro under a changing climate. *Hydrological Sciences Journal*, *60*(10), 1709–1723.

Arnell, N. W., & Gosling, S. N. (2013). The impacts of climate change on river flow regimes at the global scale. *Journal of Hydrology*, *486*, 351–364.

Arnold, J. G., Moriasi, D. N., Gassman, P. W., Abbaspour, K. C., White, M. J., Srinivasan, R., … Kannan, N. (2012). SWAT: Model use, calibration, and validation. *Transactions of the ASABE*, *55*(4), 1491–1508.

Arnold, J. G., Srinivasan, R., Muttiah, R. S., & Williams, J. R. (1998). Large area hydrologic modelling and assessment- part I: Model development. *Journal of the American Water Resources Association*, *34*(1), 73–89.

Ayaz, S. (2010). *Havza koruma eylem planlarinin hazirlanmasi projesi*. Gebze, Kocaeli: Susurluk Havzası Nihai Raporu (In Turkish).

Barry, R. G., & Chorley, R. J. (2009). *Atmosphere, weather and climate*, London and New York: Routledge.

Bozkurt, D., & Sen, O. L. (2013). Climate change impacts in the Euphrates–Tigris Basin based on different model and scenario simulations. *Journal of Hydrology*, *480*, 149–161.

Bucak, T., Trolle, D., Andersen, H. E., Thodsen, H., Erdoğan, Ş., Levi, E. E., … Beklioğlu, M. (2017). Future water availability in the largest freshwater Mediterranean lake is at great risk as evidenced from simulations with the SWAT model. *Science of the Total Environment*, *581*, 413–425.

Chattopadhyay, S., & Jha, M. K. (2016). Hydrological response due to projected climate variability in Haw River watershed, North Carolina, USA. *Hydrological Sciences Journal*, *61*(3), 495–506.

Chen, H., Xu, C. Y., & Guo, S. (2012). Comparison and evaluation of multiple GCMs, statistical downscaling and hydrological models in the study of climate change impacts on runoff. *Journal of Hydrology*, *434*, 36–45.

Clarke, L. E., Edmonds J. A., Jacoby, H. D., Pitcher, H., Reilly, J. M., & Richels, R. (2007). Scenarios of greenhouse gas emissions and atmospheric concentrations. Sub-report 2.1a of Synthesis and Assessment Product 2.1. Climate Change Science Program and the Subcommittee on Global Change Research, Washington DC.

Coxon, G., Freer, J., Westerberg, I. K., Wagener, T., Woods, R., & Smith, P. J. (2015). A novel framework for discharge uncertainty quantification applied to 500 UKgauging stations. *Water Resources Research*, *51*(7), 5531–5546.

Demircan, M., Gürkan, H., Eskioğlu, O., Arabacı, H., & Coşkun, M. (2017). Climate change projections for Turkey: Three models and two scenarios. *Turkısh Journal of Water Scıence & Management*, *1*(1), 23.

Destouni, G., Jaramillo, F., & Prieto, C. (2013). Hydroclimatic shifts driven by human water use for food and energy production. *Nature Climate Change*, *3*(3), 213–217.

Di Baldassarre, G., Wanders, N., AghaKouchak, A., Kuil, L., Rangecroft, S., Veldkamp, T. I., … Van Loon, A. F. (2018). Water shortages worsened by reservoir effects. *Nature Sustainability*, *1*(11), 617–622.

Dottori, F., Szewczyk, W., Ciscar, J. C., Zhao, F., Alfieri, L., Hirabayashi, Y., … Feyen, L. (2018). Increased human and economic losses from river flooding with anthropogenic warming. *Nature Climate Change*, *8*(9), 781–786.

Ertürk, A., Ekdal, A., Gürel, M., Karakaya, N., Guzel, C., & Gönenç, E. (2014). Evaluating the impact of climate change on groundwater resources in a small Mediterranean watershed. *Science of the Total Environment*, *499*, 437–447.

Falkenmark, M. (1989). The massive water scarcity now threatening Africa: Why isn't it being addressed? *Ambio*, *18*, 112–118.

Falkenmark, M. (2013). Gerowing water scarcity in agriculture: Future challenge to global water security. *Philosophical Transactions of the Royal Society A: Mathematical, Physical and Engineering Sciences*, *371*, 20120410.

Fowler, H. J., Blenkinsop, S., & Tebaldi, C. (2007). Linking climate change modelling to impacts studies: Recent advances in downscaling techniques for hydrological modelling. *International Journal of Climatology: A Journal of the Royal Meteorological Society*, *27*(12), 1547–1578.

Fujihara, Y., Tanaka, K., Watanabe, T., Nagano, T., & Kojiri, T. (2008). Assessing the impacts of climate change on the water resources of the Seyhan River basin in Turkey: Use of dynamically downscaled data for hydrologic simulations. *Journal of Hydrology*, *353*(1–2), 33–48.

Gampe, D., Nikulin, G., & Ludwig, R. (2016). Using an ensemble of regional climate models to assess climate change impacts on water scarcity in European river basins. *Science of the Total Environment*, *573*, 1503–1518.

Gao, X., & Giorgi, F. (2008). Increased aridity in the Mediterranean region under greenhouse gas forcing estimated from high resolution simulations with a regional climate model. *Global and Planetary Change*, *62*(3–4), 195–209.

Gaupp, F., Hall, J., & Dadson, S. (2015). The role of storage capacity in coping with intra-and inter-annual water variability in large river basins. *Environmental Research Letters*, *10*(12), 125001.

General Directorate of Water Management (GDWM). (2018). Susurluk Havzasi Taşkın Yönetim Planı Raporu, Ankara. (In Turkish).

Giorgi, F. (2006). Climate change hot-spots. *Geophysical Research Letters*, *33*(8), L08707.

Giorgi, F., & Lionello, P. (2008). Climate change projections for the Mediterranean region. *Global and Planetary Change*, *63*(2–3), 90–104.

Gorguner, M., Kavvas, M. L., & Ishida, K. (2019). Assessing the impacts of future climate change on the hydroclimatology of the Gediz Basin in Turkey by using dynamically downscaled CMIP5 projections. *Science of the Total Environment*, *648*, 481–499.

Graf, W. L. (1999). Dam nation: A geographic census of American dams and their large-scale hydrologic impacts. *Water Resources Research*, *35*(4), 1305–1311.

Graf, W. L. (2006). Downstream hydrologic and geomorphic effects of large dams on American rivers. *Geomorphology*, *79*(3-4), 336–360. http://dx.doi.org/10.1016/j.geomorph.2006.06.022.

Grill, G., Lehner, B., Thieme, M., Geenen, B., Tickner, D., Antonelli, F., … Ehalt, M. H. (2019). Mapping the world's free-flowing rivers. *Nature*, *569*(7755), 215–221.

Gupta, H. V., Sorooshian, S., & Yapo, P. O. (1999). Status of automatic calibration for hydrologic models: Comparison with multilevel expert calibration. *Journal of Hydrologic Engineering*, *4*(2), 135–143.

Haddeland, I., Heinke, J., Biemans, H., Eisner, S., Flörke, M., Hanasaki, N., … Stacke, T. (2014). Global water resources affected by human interventions and climate change. *Proceedings of the National Academy of Sciences*, *111*(9), 3251–3256.

Hagemann, S., Chen, C., Clark, D. B., Folwell, S., Gosling, S. N., Haddeland, I., … Wiltshire, A. J. (2013). Climate change impact on available water resources obtained using multiple global climate and hydrology models. *Earth System Dynamics*, *4*(1), 129–144.

Hoerling, M., Eischeid, J., Perlwitz, J., Quan, X., Zhang, T., & Pegion, P. (2012). On the increased frequency of Mediterranean drought. *Journal of Climate*, *25*(6), 2146–2161.

Holland, R. A., Scott, K. A., Flörke, M., Brown, G., Ewers, R. M., Farmer, E., … Barrett, J. (2015). Global impacts of energy demand on the freshwater resources of nations. *Proceedings of the National Academy of Sciences*, *112*(48), E6707–E6716.

Jones, B., & O'Neill, B. C. (2016). Spatially explicit global population scenarios consistent with the shared socioeconomic pathways. *Environmental Research Letters*, *11*(2016), 084003. https://doi.org/10.1088/1748-9326/11/8/084003

Jones, B., & O'Neill, B. C. (2017). Global population projection grids based on shared socioeconomic pathways (SSPs), 2010–2100. Socioeconomic Data and Applications Center. [online] Retrieved from https://doi.org/10.7927/H4RF5S0P

Karaca, M., Deniz, A., & Tayanç, M. (2000). Cyclone track variability over Turkey in association with regional climate. *International Journal of Climatology: A Journal of the Royal Meteorological Society*, *20*(10), 1225–1236.

Koç, C. (2014). A study on the development of hydropower potential in Turkey. *Renewable and Sustainable Energy Reviews*, *39*, 498–508.

Krause, P., Boyle, D. P., & Bäse, F. (2005). Comparison of different efficiency criteria for hydrological model assessment. *Advances in Geosciences*, *5*, 89–97.

Latrubesse, E. M., Arima, E. Y., Dunne, T., Park, E., Baker, V. R., d'Horta, F. M., & Ribas, C. C. (2017). Damming the rivers of the Amazon basin. *Nature*, *546*(7658), 363–369.

Lehmann, E. L., & D'Abrera, H. J. (1975). *Nonparametrics: Statistical methods based on ranks*. San Francisco, CA: Holden-Day.

Lehner, B., Verdin, K., & Jarvis, A. (2008). New global hydrography derived from spaceborne elevation data. *Eos, Transactions American Geophysical Union*, *89*(10), 93–94.

Lelieveld, J., Hadjinicolaou, P., Kostopoulou, E., Chenoweth, J., El Maayar, M., Giannakopoulos, C., … Xoplaki, E. (2012). Climate change and impacts in the eastern Mediterranean and the Middle East. *Climatic Change*, *114*(3–4), 667–687.

Magilligan, F. J., & Nislow, K. H. (2005). Changes in hydrologic regime by dams. *Geomorphology*, *71*(1–2), 61–78.

Maraun, D., & Widmann, M. (2018). *Statistical downscaling and bias correction for climate research*, Cornwall, UK: Cambridge University Press.

Meinshausen, M., Smith, S. J., Calvin, K., Daniel, J. S., Kainuma, M. L. T., Lamarque, J. F., … Thomson, A. G. J. M. V. (2011). The RCP greenhouse gas concentrations and their extensions from 1765 to 2300. *Climatic Change*, *109*(1–2), 213–241.

Monteith, J. L. (1965). Evaporation and environment. In *Symposia of the society for experimental biology* (Vol. 19, pp. 205–234). Cambridge: Cambridge University Press (CUP).

Moriasi, D. N., Arnold, J. G., Van Liew, M. W., Bingner, R. L., Harmel, R. D., & Veith, T. L. (2007). Model evaluation guidelines for systematic quantification of accuracy in watershed simulations. *Transactions of the ASABE*, *50*(3), 885–900.

Mueller Schmied, H., Adam, L., Eisner, S., Fink, G., Floerke, M., Kim, H., … Song, Q. (2016). Variations of global and continental water balance components as impacted by climate forcing uncertainty and human water use. *Hydrology and Earth System Sciences*, *20*(7), 2877–2898.

Nash, J. E., & Sutcliffe, J. V. (1970). River flow forecasting through conceptual models part I—A discussion of principles. *Journal of Hydrology*, *10*(3), 282–290.

Neitsch, S. L., Arnold, J. G., Kiniry, J. R., & Williams, J. R. (2011). Soil and water assessment tool theoretical documentation version 2009. Texas Water Resources Institute.

Oki, T., & Kanae, S. (2006). Global hydrological cycles and world water resources. *Science*, *313*(5790), 1068–1072.

Onol, B., & Semazzi, F. H. M. (2009). Regionalization of climate change simulations over the eastern Mediterranean. *Journal of Climate*, *22*(8), 1944–1961.

Ozturk, M. Z., Cetinkaya, G., & Aydin, S. (2017). Climate types of Turkey according to Klippen-Geiger climate classification. *Journal of Geography-Cografya Dergısı*, *35*, 17–27.

Ozturk, T., Ceber, Z. P., Türkeş, M., & Kurnaz, M. L. (2015). Projections of climate change in the Mediterranean Basin by using downscaled global climate model outputs. *International Journal of Climatology*, *35*(14), 4276–4292.

Ozturk, T., Türkeş, M., & Kurnaz, L. (2011). RegCM4. 3.5. Analysing projected changes in future air temperature and precipitation climatology of

Turkey by using RegCM4.3.5 climate simulations. *Aegean Geographical Journal*, *20*(1), 17–27 (in Turkish with an English abstract, figure and table captions).

Partal, T., & Kahya, E. (2006). Trend analysis in Turkish precipitation data. *Hydrological Processes*, *20*(9), 2011–2026.

Peel, M. C., Finlayson, B. L., & McMahon, T. A. (2007). Updated world map of the Köppen-Geiger climate classification. *Hydrology and Earth System Sciences*, *11*, 1633–1644.

Poff, N. L., Olden, J. D., Merritt, D. M., & Pepin, D. M. (2007). Homogenization of regional river dynamics by dams and global biodiversity implications. *Proceedings of the National Academy of Sciences*, *104*(14), 5732–5737.

Riahi, K., Grübler, A., & Nakicenovic, N. (2007). Scenarios of long-term socio-economic and environmental development under climate stabilization. *Technological Forecasting and Social Change*, *74*(7), 887–935.

Rockström, J., Falkenmark, M., Karlberg, L., Hoff, H., Rost, S., & Gerten, D. (2009). Future water availability for global food production: The potential of green water for increasing resilience to global change. *Water Resources Research*, *45*(7), W00A12.

Samaniego, L., Thober, S., Kumar, R., Wanders, N., Rakovec, O., Pan, M., … Marx, A. (2018). Anthropogenic warming exacerbates European soil moisture droughts. *Nature Climate Change*, *8*(5), 421–426.

Sen, B., Topcu, S., Türkeş, M., Sen, B., & Warner, J. F. (2012). Projecting climate change, drought conditions and crop productivity in Turkey. *Climate Research*, *52*, 175–191.

Smith, S. J., & Wigley, T. M. L. (2006). Multi-gas forcing stabilization with Minicam. *The Energy Journal*, *27*(Special Issue 3), 373–391.

Soil Conservation Service . (1993). *Hydrology*, *national engineering handbook*, *supplement A*, *section 4*. Chap. 10. Washington, DC: Soil Conservation Service, USDA.1956, 1964, 1971, 1985

Stehr, A., Debels, P., Romero, F., & Alcayaga, H. (2008). Hydrological modelling with SWAT under conditions of limited data availability: Evaluation of results from a Chilean case study. *Hydrological Sciences Journal*, *53*(3), 588–601.

Stocker, T. F., Qin, D., Plattner, G. K., Tignor, M. M., Allen, S. K., Boschung, J., … Midgley, P. M. (2013). Climate change 2013: The physical science basis. Contribution of working group I to the fifth assessment report of the intergovernmental panel on climate change.

Sunde, M. G., He, H. S., Hubbart, J. A., & Urban, M. A. (2017). Integrating downscaled CMIP5 data with a physically based hydrologic model to estimate potential climate change impacts on streamflow processes in a mixed-use watershed. *Hydrological Processes*, *31*(9), 1790–1803.

Tatli, H., Nüzhet, D. H., & Mentes, S. Ş. (2004). A statistical downscaling method for monthly total precipitation over Turkey. *International Journal of Climatology: A Journal of the Royal Meteorological Society*, *24*(2), 161–180.

Türkeş, M., Yozgatlıgil, C., Batmaz, İ., İyigün, C., Koç, E. K., Fahmi, F. M., & Aslan, S. (2016). Has the climate been changing in Turkey? Regional climate change signals based on a comparative statistical analysis of two consecutive time periods, 1950-1980 and 1981-2010. *Climate Research*, *70*(1), 77–93.

Turkish Statistical Institute-TURKSTAT (2018). www.tuik.gov.tr.

Turp, M. T., Öztürk, T., Türkeş, M., & Kurnaz, M. L. (2014). RegCM4. 3.5 bölgesel iklim modelini kullanarak Türkiye ve çevresi bölgelerin yakın gelecekteki hava sıcaklığı ve yağış klimatolojileri için öngörülen değişikliklerin incelenmesi. *Ege Coğrafya Dergisi*, *23*(1), 1–24 (In Turkish).

Van Vuuren, D. P., Edmonds, J., Kainuma, M., Riahi, K., Thomson, A., Hibbard, K., … Masui, T. (2011). The representative concentration pathways: An overview. *Climatic Change*, *109*(1–2), 5–31.

Vörösmarty, C. J., Douglas, E. M., Green, P. A., & Revenga, C. (2005). Geospatial indicators of emerging water stress: An application to Africa. *Ambio: A Journal of the Human Environment*, *34*(3), 230–236.

Vörösmarty, C. J., Green, P., Salisbury, J., & Lammers, R. B. (2000). Global water resources: Vulnerability from climate change and population growth. *Science*, *289*(5477), 284–288.

Wilby, R. L., & Wigley, T. M. L. (1997). Downscaling general circulation model output: A review of methods and limitations. *Progress in Physical Geography*, *21*(4), 530–548.

Wise, M., Calvin, K., Thomson, A., Clarke, L., Bond-Lamberty, B., Sands, R., … Edmonds, J. (2009). Implications of limiting CO2 concentrations for land use and energy. *Science*, *324*(5931), 1183–1186.

Wood, A. W., Leung, L. R., Sridhar, V., & Lettenmaier, D. P. (2004). Hydrologic implications of dynamical and statistical approaches to downscaling climate model outputs. *Climatic Change*, *62*(1–3), 189–216.

Yuksel, I. (2015). Water management for sustainable and clean energy in Turkey. *Energy Reports*, *1*, 129–133.

Zeng, S., Xia, J., She, D., Du, H., & Zhang, L. (2012). Impacts of climate change on water resources in the Luan River basin in North China. *Water International*, *37*(5), 552–563.

SUPPORTING INFORMATION

Additional supporting information may be found online in the Supporting Information section at the end of this article.

How to cite this article: Akbas A, Freer J, Ozdemir H, Bates PD, Turp MT. What about reservoirs? Questioning anthropogenic and climatic interferences on water availability. *Hydrological Processes*. 2020;34:5441–5455. https://doi.org/10.1002/hyp.13960